

Food Science and Human Wellness  
食品科学与人类健康(英文)  
ISSN 2213-4530,CN 10-1750/TS

## 《Food Science and Human Wellness》网络首发论文

题目: Lycii Radicis Cortex suppresses the growth of non-small cell lung cancer via enhancing the anti-tumor immunity

作者: Heng Yin, Meng Liu, Yaling Zhao, Haitao Wu, Danna Zheng, Zhenhui Guo, Ying Zhou, Shaofeng Wu, Chuanbing Chen, Lei Zhang, Shanshan Song, Yanli He, Ren Zhang

收稿日期: 2023-03-23

网络首发日期: 2023-10-12

引用格式: Heng Yin, Meng Liu, Yaling Zhao, Haitao Wu, Danna Zheng, Zhenhui Guo, Ying Zhou, Shaofeng Wu, Chuanbing Chen, Lei Zhang, Shanshan Song, Yanli He, Ren Zhang. Lycii Radicis Cortex suppresses the growth of non-small cell lung cancer via enhancing the anti-tumor immunity[J/OL]. Food Science and Human Wellness. <https://link.cnki.net/urlid/10.1750.TS.20231010.1411.006>



**网络首发:** 在编辑部工作流程中,稿件从录用到出版要经历录用定稿、排版定稿、整期汇编定稿等阶段。录用定稿指内容已经确定,且通过同行评议、主编终审同意刊用的稿件。排版定稿指录用定稿按照期刊特定版式(包括网络呈现版式)排版后的稿件,可暂不确定出版年、卷、期和页码。整期汇编定稿指出版年、卷、期、页码均已确定的印刷或数字出版的整期汇编稿件。录用定稿网络首发稿件内容必须符合《出版管理条例》和《期刊出版管理规定》的有关规定;学术研究成果具有创新性、科学性和先进性,符合编辑部对刊文的录用要求,不存在学术不端行为及其他侵权行为;稿件内容应基本符合国家有关书刊编辑、出版的技术标准,正确使用和统一规范语言文字、符号、数字、外文字母、法定计量单位及地图标注等。为确保录用定稿网络首发的严肃性,录用定稿一经发布,不得修改论文题目、作者、机构名称和学术内容,只可基于编辑规范进行少量文字的修改。

**出版确认:** 纸质期刊编辑部通过与《中国学术期刊(光盘版)》电子杂志社有限公司签约,在《中国学术期刊(网络版)》出版传播平台上创办与纸质期刊内容一致的网络版,以单篇或整期出版形式,在印刷出版之前刊发论文的录用定稿、排版定稿、整期汇编定稿。因为《中国学术期刊(网络版)》是国家新闻出版广电总局批准的网络连续型出版物(ISSN 2096-4188, CN 11-6037/Z),所以签约期刊的网络版上网络首发论文视为正式出版。



Contents lists available at CNKI

Food Science and Human Wellness

journal homepage: <http://www.keaipublishing.com/en/journals/food-science-and-human-wellness>



## *Lycii Radicis Cortex* suppresses the growth of non-small cell lung cancer via enhancing the anti-tumor immunity

Heng Yin<sup>a,1</sup>, Meng Liu<sup>a,1</sup>, Yaling Zhao<sup>a,1</sup>, Haitao Wu<sup>b</sup>, Danna Zheng<sup>f</sup>, Zhenhui Guo<sup>a</sup>, Ying Zhou<sup>a</sup>, Shaofeng Wu<sup>a</sup>, Chuanbing Chen<sup>c</sup>, Lei Zhang<sup>c</sup>, Shanshan Song<sup>d\*</sup>, Yanli He<sup>e\*</sup>, Ren Zhang<sup>a\*</sup>

<sup>a</sup> Research Centre of Basic Intergrative Medicine, School of Basic Medical Sciences, Guangzhou University of Chinese Medicine, Guangzhou 510006, China

<sup>b</sup> Science and Technology Innovation Center, Guangzhou University of Chinese Medicine, Guangzhou 510006, China

<sup>c</sup> School of Pharmaceutical Sciences, Guangzhou University of Chinese Medicine, Guangzhou 510006, China

<sup>d</sup> Integrated Hospital of Traditional Chinese Medicine, Southern Medical University, Guangzhou 510315, China

<sup>e</sup> Department of Pathology and Pathophysiology, School of Basic Medical Sciences, Guangzhou University of Chinese Medicine, Guangzhou 510006, China

<sup>f</sup> The First Affiliated Hospital of Jinan University, Guangzhou 510006, China

**ABSTRACT:** *Lycii Radicis Cortex* (LRC) is a medicinal and food homologous plant with various pharmacological activities, including anti-tumor effects. This study explores the anti-tumor effect of LRC on non-small cell lung cancer (NSCLC) and its molecular mechanism using mice bearing Lewis lung carcinoma cells. LRC significantly suppressed the growth of NSCLC. Besides, RNA sequencing of mice tumors and hematoxylin & eosin and immunofluorescence staining revealed that LRC promoted the infiltration of T lymphocytes, specifically GZMB<sup>+</sup>CD8<sup>+</sup>T lymphocytes, in tumor tissues. The Gene Set Enrichment Analysis of spleen RNA indicated that LRC up-regulated PD-1-downstream pathways, suggesting that LRC exerted its effects through the PD-L1/PD-1 pathway. Further experiments revealed that LRC interacted with PD-L1, blocking PD-L1/PD-1 binding and thus restoring the T cell killing activity on tumor cells. Together, these results support using LRC as healthy food to improve anti-tumor immunity in patients with NSCLC.

**Keywords:** *Lycii Radicis Cortex*; Non-small cell lung cancer; PD-L1; Immune Checkpoint.

### 1. Introduction

Non-small cell lung cancer (NSCLC) accounts for more than 80% of lung cancer cases, which remain the top cause of cancer-related death in China and worldwide [1]. Patients with advanced NSCLC typically have a poor prognosis and an overall five-year survival rate of only about 5% [2]. As it is a refractory cancer, treating lung cancer is fraught with challenges. After conventional radiotherapy and chemotherapy, immunotherapy has redefined the way cancer is treated. Dietary supplements, which are often used to prevent cancer, slow down cancer progression, or improve immunity, are a promising adjunct strategy [3-5].

<sup>1</sup> These authors contributed equally to this work.

\*Corresponding author

zren@gzucm.edu.cn (Ren Zhang); blhhh@gzucm.edu.cn (Yanli He);  
songshanshan2007@163.com (Shanshan Song)

Received 23 March 2023

Received in revised form 23 June 2023

Accepted 27 July 2023

*Lycii Radicis Cortex* (LRC) is the dried root bark of *Lycium Chinese Mill.*, traditionally used to prepare porridge, soup, and wine. It has been used as medicine in China for hundreds of years and was included in the list of “homologous medicine and food” by the Chinese Ministry of Health in 2002. Modern pharmacological studies have revealed that LRC and its components have many pharmacological activities, such as antiviral, antibacterial, hypolipidemic, hypotensive, hypoglycemic, and anti-tumor effects [6]. Currently, the anticancer properties of LRC are under-documented. A handful of studies have demonstrated that LRC can promote apoptosis in glioma cells and inhibit the growth of glioma in animal tumor models [7]. However, its effects on other types of cancer have not been reported. To date, more than 130 ingredients have been isolated from LRC, including alkaloids, flavonoids, phenylpropanoid, anthraquinones, terpenoids, and sterols [8]. Alkaloids are the most important active components in LRC and have many structural types. Kukoamine A and B, two amide alkaloids isomers, are the representative components of LRC [9]. Kukoamine A and B have various pharmacological activities, including antioxidant, anti-inflammatory, neuroprotective, and hypoglycemic effects [10]. Kukoamine A can also directly induce glioblastoma cell apoptosis and inhibit tumor growth and metastasis [11]. Apigenin, a dietary flavonoid compound isolated from LRC, has a wide range of biological activities, especially anti-tumor effects. In lung cancer, apigenin not only directly inhibits cell growth or induces apoptosis, but also inhibits angiogenesis, enhances chemotherapy sensitivity, and promotes anti-tumor immune response [12]. Linarin is also a dietary flavonoid with significant anti-inflammatory activity in LRC, and it inhibits the growth and invasion of lung cancer cells [13]. Linarin and apigenin strongly support the “homologous medicine and food” character of LRC.

LRC is a component of the classical prescription Xie Bai Sai, used to treat lung cancer in China [14]. However, it remains unclear whether LRC can suppress the growth of NSCLC and its underlying mechanism. In this study, we explored the inhibitory effect of LRC on lung cancer by employing a mouse model using Lewis lung carcinoma (LLC) cells and studied the related mechanism.

## 2. Methods

### 2.1. Cell culture

NSCLC cell line A549, Jurkat (E6-1) T cells, and Lewis cells were purchased from American Type Culture Collection (ATCC). All cells were cultured in RPMI1640 medium (Gibco, Pittsburgh, PA, USA) supplemented with 10% fetal bovine serum (FBS) (Thermo Fisher Scientific, Brazil). The cells were grown in a humidified atmosphere at 37 °C in 5% CO<sub>2</sub>. A549 cells were lentivirally (Shanghai Genechem Co., Ltd.) transduced to stably express human programmed cell death ligand 1 (PD-L1) (hereafter named A549-PD-L1-OE cells), and an empty lentiviral vector was used as a negative control (resulting in A549-NC cells). The efficiency of PD-L1 overexpression was assessed by western blot following puromycin (Beyotime, ST551) selection. Human Peripheral blood mononuclear cells (PBMC) were obtained from heparinized blood from healthy donors, cultured *in vitro*, and activated using CD3 anti-human antibody (BioLegend, 317301, 100 ng/mL), CD28 anti-human antibody (BioLegend, 302901, 100 ng/mL) and interleukin-2 (IL-2) (BioLegend, 10 ng/mL) for 24 h. Western blot was used to determine the optimal concentration of

phytohemagglutinin (PHA) (yuanyebio, S12056) to stimulate the expression of programmed death 1 (PD-1) in Jurkat T cells.

## 2.2. Preparation for extracts of *Lycii Radicis Cortex*

We kept a voucher specimen (LRC202008) of the LRC in our laboratory for future reference. We prepared and controlled the quality of LRC as we previously described [15]. In short, the dried LRC (2000 g) was ground into powder and soaked in 20 L of 95% ethanol (24 h, twice). The extract solutions were then combined, filtered, concentrated under reduced pressure, and then lyophilized (Guangzhou Dexiang Technology Co., Ltd., Guangzhou, China). The obtained powder (160.5 g) was dissolved in RPMI1640 medium or phosphate-buffered saline (PBS) (Gibco, USA). Before use, the LRC solution was filtered with a 0.22  $\mu\text{m}$  microporous filter membrane to remove insoluble matter. The production batch of LCR used in this study was the same as in our previous report [15], which contained the HPLC (Shimadzu (Suzhou) Instruments Manufacturing Co., Ltd., Suzhou, China) analysis of flavonoids in LRC.

## 2.3. In vivo LRC treatment

Six-week-old male C57BL/6J mice were obtained from the Laboratory Animal Center of the Guangzhou University of Traditional Chinese Medicine. The animal experiments and protocols were approved by the Guangzhou University of Chinese Medicine (Approval ID: 20220529001). Tumor-bearing mice were prepared by the subcutaneous inoculation of  $10^6$  Lewis cells per C57BL/6 mouse. Three days after the inoculation, the mice were randomly divided into four groups (6 mice/group). As soon as the resulting tumor was detectable by palpation, the mice received normal saline, 2 or 8 g/kg LRC by gavage, or 200  $\mu\text{L}$  cyclophosphamide (30 mg/kg) by intraperitoneal injection once daily for 15 days. The tumor length and width were measured with a vernier caliper at the same time every day, and the mice were weighed. The tumor volume calculation formula was  $V = \text{length} \times \text{width}^2/2$ , and the tumor growth curves were drawn along. Mice were euthanized by cervical dislocation, and the resulting tumors, major organs, and blood samples were harvested for subsequent analyses. The organ index was calculated using the following formula: Organ Index = Organ Weight (mg) / Body Weight (g). A fraction of retrieved tumor was fixed in 4% paraformaldehyde and stained with Hematoxylin and Eosin (H&E). Images were captured using a microscope (Olympus, Japan, BX43). The total RNA of remaining tumor tissue and spleen was extracted for Next-Generation Sequencing.

## 2.4. Enzyme-Linked Immune Assay (ELISA)

Serum was prepared using a standard protocol. The serum IL-2 and interferon- $\gamma$  (IFN- $\gamma$ ) concentrations were determined by ELISA. ELISA detection was performed using an ELISA kit (Jiangsu Meimian industrial Co.,Ltd). Briefly, the serum was incubated in a 96-well plate with wells coated with the designated antibodies, and the absorbance at 450 nm was measured using a microplate reader. All samples were replicated three times.

## 2.5. Flow Cytometry

Mice spleens were collected and mechanically disaggregated using a 40 µm cell filter. For splenocyte suspensions, erythrocytes were removed using a red blood cell lysis buffer (biosharp). The cells were stained with the following antibodies (obtained from Biolegend) and incubated at 4 °C for 0.5 h: FITC anti-mouse CD3 antibody (Cat No: 100305), BV510 anti-mouse CD8a antibody (Cat No:562952), APC/Cy7 anti-mouse CD4 antibody (Cat No: 100525). Flow cytometry was performed with a BD Fortessa apparatus, and data were analyzed with FlowJo V10.

## 2.6. Immunofluorescence

Paraffin-embedded tumor sections were cut into 4 µm sections. Then the slides were deparaffinized and rehydrated, and antigen retrieval was performed. The tissue was permeabilized/blocked with 0.5% Triton 100 × (Shanghai Biyuntian Biotechnology, ST797) and normal goat serum (ZSGB, ZLI-9022) for 60 min at 25 °C. Staining was carried out with the following fluorochrome-conjugated antibodies: BV510 anti-mouse CD8a antibody (Biolegend, Cat No:562952) and APC anti-mouse Granzyme B antibody (Biolegend, Cat No: 372203). All immunofluorescence sections were counterstained with DAPI (Shanghai Biyuntian Biotechnology, C1005) to identify total cell nuclei and visualized by immunofluorescence microscopy.

## 2.7. RNA sequencing analysis

The RNA library construction and sequencing of mice spleen and tumor (from the 2 g/kg LRC and control groups) were carried out by Novogene (Novogene, Guangzhou, China). Illumina sequencing was performed on each sample according to standard sequencing protocol. The original measurements were pruned to produce clean data, which were then compared with the reference genome (GRCm39). The correlation between LRC and immune infiltration was analyzed using the TIMER database (<https://cistrome.shinyapps.io/timer/>). As mentioned earlier, Gene Set Enrichment Analysis (GSEA) was performed using the local version of GSEA tools (<http://www.broadinstitute.org/gsea/index.jsp>) [16]. Gene Ontology (GO) and Kyoto Encyclopedia of Genes and Genomes (KEGG) pathway enrichment analysis were conducted using the DAVID Bioinformatics Resources (<https://david.ncifcrf.gov/>).

## 2.8. Homogeneous Time-Resolved Fluorescence (HTRF) Assay

According to the instructions of the HTRF kit (Cisbio, NO: 63ADK000CPAPEG) manufacturer, the corresponding reagents and LRC were added to HTRF special 96-well plates in sequence, and incubated for 4 h at room temperature and away from light. The fluorescence intensity of each well at 665 nm and 615 nm was read using a Tecan Infinite M1000 PRO microplate reader, and the HTRF Ratio (665 nm emission / 615 nm emission) was obtained. The HTRF Ratio was calculated for each LRC concentration according to the formula:  $\text{HTRF Ratio} = \text{Signal } 665 \text{ nm} / \text{Signal } 620 \text{ nm} \times 10000$ . Then, GraphPad Prism 8.0 was used for curve fitting, and the half-maximal inhibitory concentration (IC<sub>50</sub>) was calculated.

### 2.9. Biolayer interferometry (BLI) analysis of PD-L1-LRC interactions (PD-L1 binding assay)

The binding affinity ( $K_D$ ) of LRC to PD-L1 was determined using biolayer inference (BLI) on an Octet Red9e non-standard machine interaction analysis system (ForteBio). Binding experiments were performed in a binding buffer (PBS, 0.02% Tween 20, 0.1% BSA, 10 mmol/L glycine, pH 2.0) at 37 °C. The sensor was loaded with biotinylated PD-L1 protein in 96 wells and eluted in the buffer for 60 s until the curve stabilized. Reactions were then performed in sample LRC wells (at concentrations of 0.0603, 0.3015, 1.51, 7.54, 37.7, 188.4, and 942.2 nmol/L). Then, the resulting mixture was immersed in binding buffer wells for 120 s to allow complete dissociation. The constants are determined using the dynamic analysis model.

### 2.10. PBMC-mediated cancer cell killing assay

In a 96-well plate, 8000 A549-PD-L1-OE or A549-NC cells were co-cultured with 5000 activated PBMCs. A549-PD-L1-OE cells with PBMCs were treated with LRC (0, 4, or 12  $\mu\text{g}/\text{mL}$ ). After incubation for 12 h, the supernatant was aspirated, and the adhered cells were stained with 1  $\mu\text{g}/\text{mL}$  Propidium Iodide (PI) (Shanghai Biyuntian Biotechnology Co., Ltd., ST511) and 1  $\mu\text{g}/\text{mL}$  Hoechst 33342 (Shanghai Biyuntian Biotechnology Co., Ltd., C1022). Four fields of view from each well were selected randomly to take pictures under a fluorescence microscope. Image J software was used to count blue cells (Hoechst33342-stained cells, total tumor cells), and red cells (PI-stained cells, apoptotic tumor cells). The killing rate of PBMC to tumor cells was calculated using the following formula: killing rate = number of apoptotic tumor cells (red fluorescence) / all the tumor cells in the field of vision (blue fluorescence)  $\times$  100%.

### 2.11. Apoptosis assay

Jurkat T cells were stimulated with 2  $\mu\text{g}/\text{mL}$  phytohemagglutinin (PHA) for 24 h to produce PD-1. After being washed with PBS, 200,000 activated Jurkat T cells were put into a 6-well plate and incubated with 1  $\mu\text{g}/\text{mL}$  PD-L1 protein and LRC (0, 4, or 12  $\mu\text{g}/\text{mL}$ ) for 20 h. Finally, Jurkat T cells were stained with the apoptosis kit (Shanghai Biyuntian Biotechnology, C1062M) and then apoptotic cells were counted by flow cytometry.

### 2.12. Proliferation inhibition assay

Fresh PBMCs (20,000 cells/well) and LRC (0, 12, 36, or 108  $\mu\text{g}/\text{mL}$ ) were seeded in a 96-well plate and incubated for 72 h. CellTiter-Lumi™ Steady Luminescence Assay Reagent (50  $\mu\text{L}$ ) was added to accelerate the cell lysis and the plate was shaken for 120 s, then incubated at 25 °C for 600 s. Chemiluminescence was quantified using a multi-function microplate reader with a detection time of 0.25–1 s. The calculation formula of cell vitality was: Luminescence readout (treated cells) / Luminescence readout (control cells).

Jurkat T cells or LLC cells (20,000 cells/well) were seeded in a 96-well plate and incubated with LRC at various final concentrations for 24 h. The cell viability was measured using a cell counting kit-8 (meilunbio) in accordance with the manufacturer's instructions. After incubation for 30 min, the absorbance at 450 nm per well was measured to calculate the cell survival rate.

### 2.13. Western Blot Analysis

The treated Jurkat T cells were harvested, lysis buffer and protease inhibitor were added, and cells were lysed on ice for 30 min. A BCA protein concentration detection kit (Beyotime, p0011) was used to quantify total proteins. The proteins (20  $\mu$ g in solution) were separated by molecular weight using 8% or 10% SDS-PAGE. The proteins were then transferred from the gel to the pure nitrocellulose membrane. To avoid nonspecific binding of the antibody, the membrane was blocked by bathing in 5% non-fat milk. Next, the blots were incubated overnight at 4 °C with the primary antibody. The primary antibody was recycled and the membrane was washed with TBST before incubation with the secondary antibodies (goat anti-rabbit secondary (cell signaling, 7074s) and goat anti-mouse secondary (BBI, D110087-0100)) at 25 °C for 120 min. Protein bands were evenly coated with an electrochemiluminescence solution, exposed, and photographed using a chemiluminescent imaging system. The primary antibodies were phospho Src homology-2 domain-containing protein-tyrosine phosphatase-2 (p-SHP2) (Affinity Biosciences, AF3412), Caspase 3 (Cell Signaling, 9665s), PD-1 (Proteintech, 66220-1-Ig), and GAPDH (BBI, D110087-0100).

### 2.14. Statistics

Normal distribution was assessed using the Shapiro-Wilk test. Normally distributed data was expressed as mean  $\pm$  standard deviation (SD). Groups were compared using *t*-test or one-way ANOVA. The median (interquartile range) and Kruskal–Wallis rank sum test were used for non-normally distributed data. A *P* value  $\leq 0.05$  was considered statistically significant. All statistical analyses were performed using GraphPad Prism 8 and SPSS 25.0.

## 3. Results

### 3.1. LRC effectively suppressed tumor growth *in vivo*

The animal experiments revealed that LRC dramatically reduced the tumor volume (Fig. 1A, Fig. 1C) and weight (Fig. 1B). The anti-tumor effect of LRC was not accompanied with significant weight loss (Fig. 1D). The H&E staining of the liver and kidney demonstrated the absence of toxicity from LRC treatment (Fig. 1E), indicating an acceptable tolerance for LRC. Meanwhile, LRC could not suppress the LLC cell proliferation *in vitro* (Fig. 1F). Our previous report revealed that LRC did not suppress the proliferation of the NSCLC cell lines A549 and H1299 [15]. These results indicate that the inhibition of NSCLC progression in LLC-bearing mice was not due to the tumor-selective cytotoxicity of LRC and suggest that LRC could exert its anti-tumor effect through the immune response.

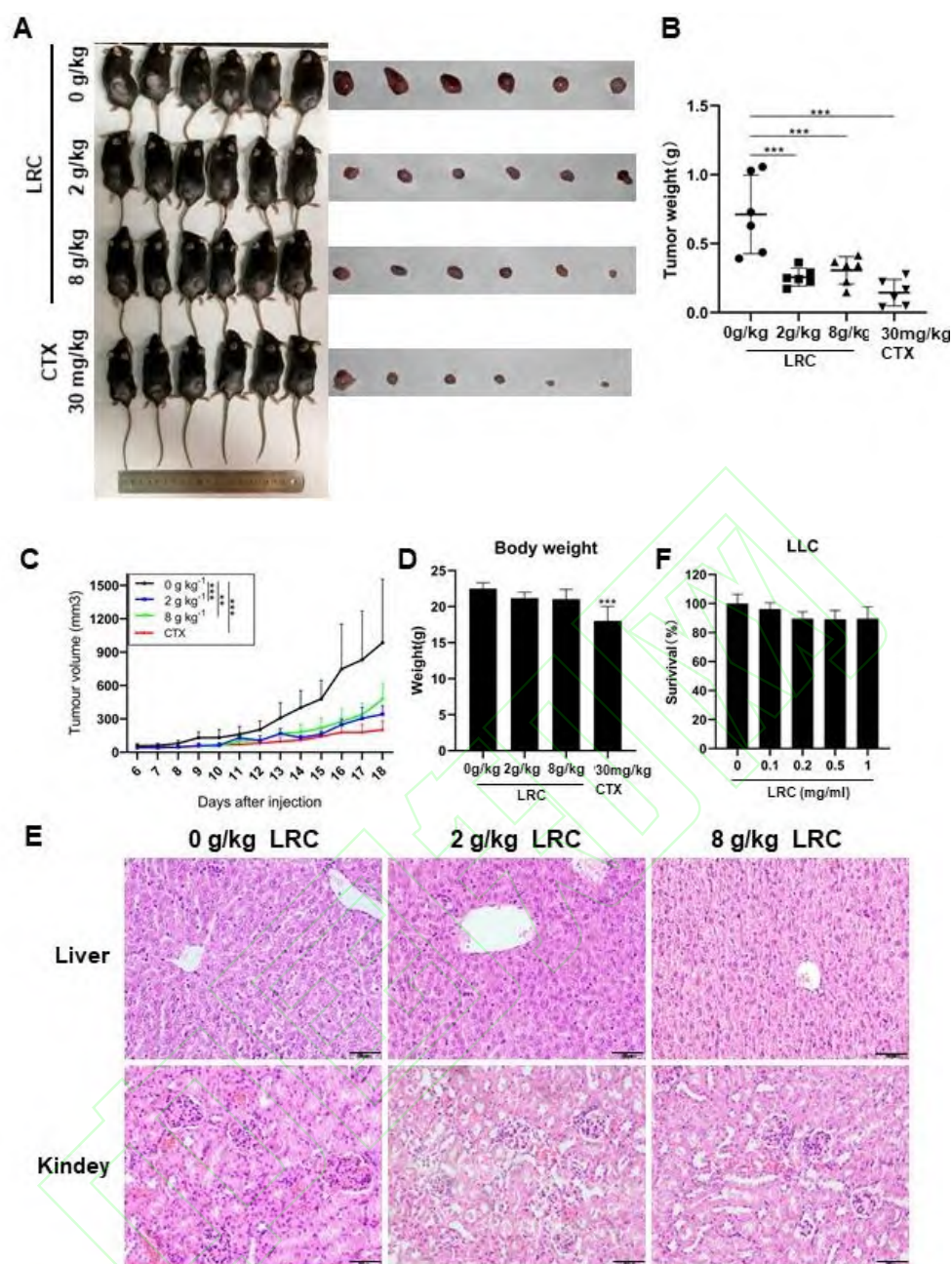


**Fig1.** LRC suppresses the growth of lung cancer in mice. Three days after the subcutaneous inoculation with Lewis lung carcinoma (LLC) cells, C57BL/6J mice received LRC (2 or 8 g/kg per day) by gavage or cyclophosphamide (CTX) by intraperitoneal injection for 15 days. (A) The mice bearing LLC tumors and the excised tumors from sacrificed mice. (B) Tumor weight from LLC-bearing mice treated with LRC or CTX. (C) Tumor volume growth curve of mice treated with LRC or CTX. (D) Effects of treatment mode and dose on the body weight of mice. (E) Pathological sections of kidney and liver obtained from mice bearing LLC tumors. Organs were stained with Hematoxylin and Eosin (H&E), and representative images were captured. (F) Effect of LRC on LLC cell proliferation *in vitro*. These data were presented as the mean  $\pm$  SD, \*\*  $P < 0.01$ , \*\*\*  $P < 0.001$  vs. control group,  $n = 6$ .

### 3.2. LRC enhanced the host's anti-tumor immune response

To examine the effect of LRC on the anti-tumor immune response, we first investigated the immune organs of each group of mice, and found that LRC had no noticeable impact on the weight of the spleen (Fig. 2A) and thymus (Fig. 2B). The flow cytometry analysis revealed an inconspicuous difference in the percentage of CD4<sup>+</sup> T lymphocytes and CD8<sup>+</sup> T lymphocytes in the spleen of control and LCC-treated mice (Supporting Information A). However, ELISA results indicated that mice treated with a high LRC dose had

noticeably higher levels of serum IL-2 and IFN- $\gamma$  (which are associated with T lymphocytes activity) than the control groups (Fig. 2C, Fig. 2D). To further explore the effect of LRC on immunity, we sequenced the RNA of the mice spleens. The principal component analysis (Supporting Information B) and correlation analysis (Supporting Information C) of RNA sequencing results showed that our samples exhibited good repeatability. Comparing data of the LRC-treated mice with that of the control mice revealed 5107 differentially expressed genes (DEGs) (2180 up-regulated and 2927 downregulated genes; Fig. 2E). The top 100 DEGs are shown in Supporting Information Table 1. The hierarchical cluster analysis indicated that mice treated with 2 g/kg LRC had significantly altered gene expression profiles (Fig. 2F). In the RNA sequencing data, we found that LRC significantly up-regulated CD40 ligand (CD40lg), zeta chain of T cell receptor-associated protein kinase 70 (Zap70), lymphocyte cell-specific protein-tyrosine kinase (Lck), and tumor necrosis factor (TNF), which are proteins involved in T cell activation (Fig. 2G). Therefore, we performed GO, KEGG pathway enrichment analyses (Supporting Information Table 2 - Table 3) and GSEA on the RNA sequencing data of the spleen and found that LRC treatment was significantly related to the up-regulation of the T cell receptor (TCR) signaling pathway and Leukocyte transendothelial migration pathway (Fig. 2H, Fig. 2I). These results indicate that LRC plays an important role in the immune response and suggest that LRC induces the migration of some activated lymphocytes to the tumor.

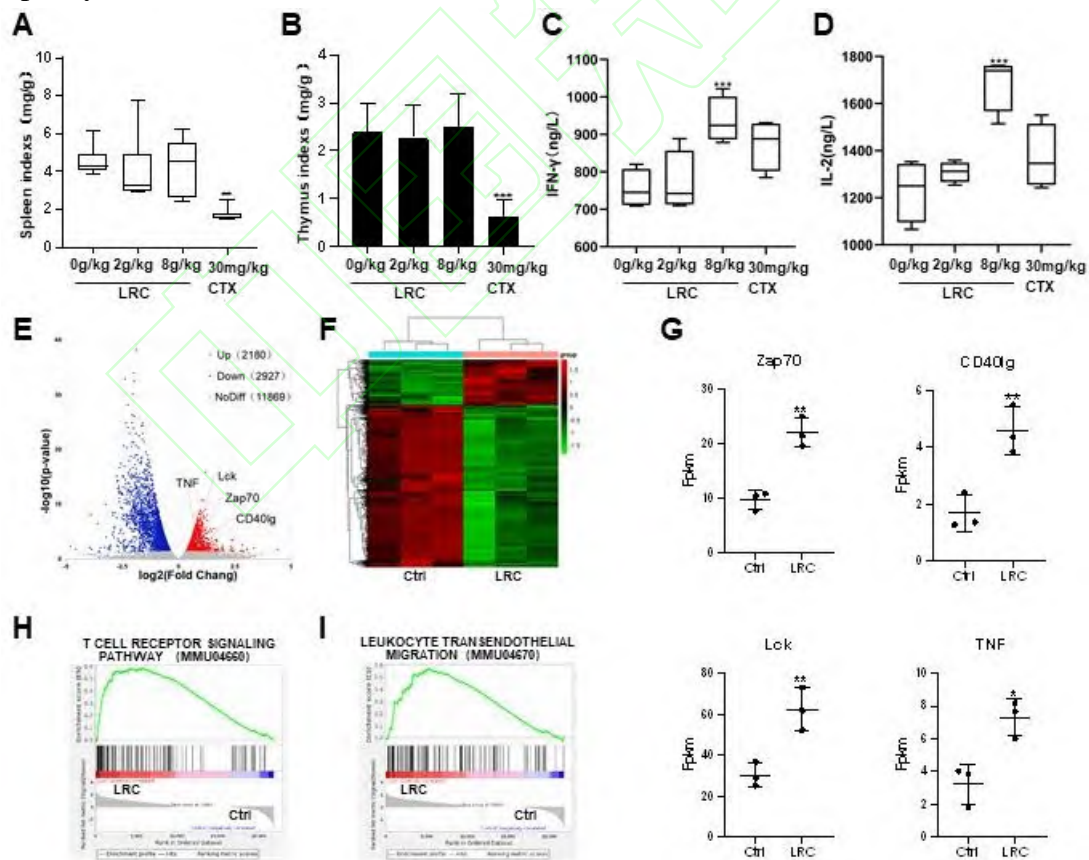


**Fig2.** LRC enhanced the host anti-tumor immune response. (A) Spleen indices in CTX- or LRC-treated mice. (B) Thymus indices in CTX- or LRC-treated mice. ELISA results showing levels of IFN- $\gamma$  (C) and IL-2 (D) in the serum of LRC-treated tumor-bearing mice compared with control mice (Ctrl). (E) Volcano plot showing the differentially expressed genes in the spleen of LRC-treated mice and control mice. The red and blue dots indicate significantly up-regulated and downregulated genes, respectively, in the LRC-treated group. (F) Heatmap and Hierarchical clustering analysis of differentially expressed genes in the Ctrl and LRC groups. (G) The expression of CD40lg, Zap70, Lck, and TNF in the RNA sequencing data of the Ctrl and LRC-treated mice spleen. GSEA showed that LRC activated the T cell receptor signaling pathway (H) and Leukocyte

transendothelial migration pathway (I) in mice spleen. Measurement data are represented by M (P25 to P75) or mean  $\pm$ SD, \*  $P < 0.05$ , \*\*  $P < 0.01$ , \*\*\*  $P < 0.001$  vs. control group.

### 3.3. LRC promotes CD8<sup>+</sup> T Cell infiltration and activity in tumors

To explore whether LRC induced the migration of lymphocytes to the tumor tissue, we sequenced the RNA of the tumors and quantified the tumor-infiltrating lymphocytes (TILs). The H&E staining revealed a remarkable increase of TILs in LRC-treated tumor tissues (Fig. 3A). Meanwhile, the immunoinfiltration analysis of the RNA sequencing data of tumor tissues using the TIMER database showed that LRC promoted CD8<sup>+</sup> T cell infiltration (Fig. 3B, Fig. 3C). The GSEA of the tumor RNA sequencing data revealed that LRC promoted the IL-12 family signaling pathway and negatively regulated the T cell apoptotic process (Fig. 3D, Fig. 3E). As IL-12 is involved in the infiltration of immune effector cells [17], these results confirmed that LRC enhanced TILs in tumors and suggested that LRC could reduce T cell apoptosis. To confirm that, we used immunofluorescence and found that LRC promoted GZMB<sup>+</sup>CD8<sup>+</sup> T lymphocytes infiltration into tumor tissues (Fig. 3F, Fig. 3G). Supporting Information Table 4 lists the top 100 DEGs of tumors in Control and LRC-treated mice. The results of KEGG and GO pathway enrichment analyses are presented in the Supporting Information Table 5 - Table 6. Altogether, these results show that LRC promotes the infiltration and activity of CD8<sup>+</sup> T cells in tumors.

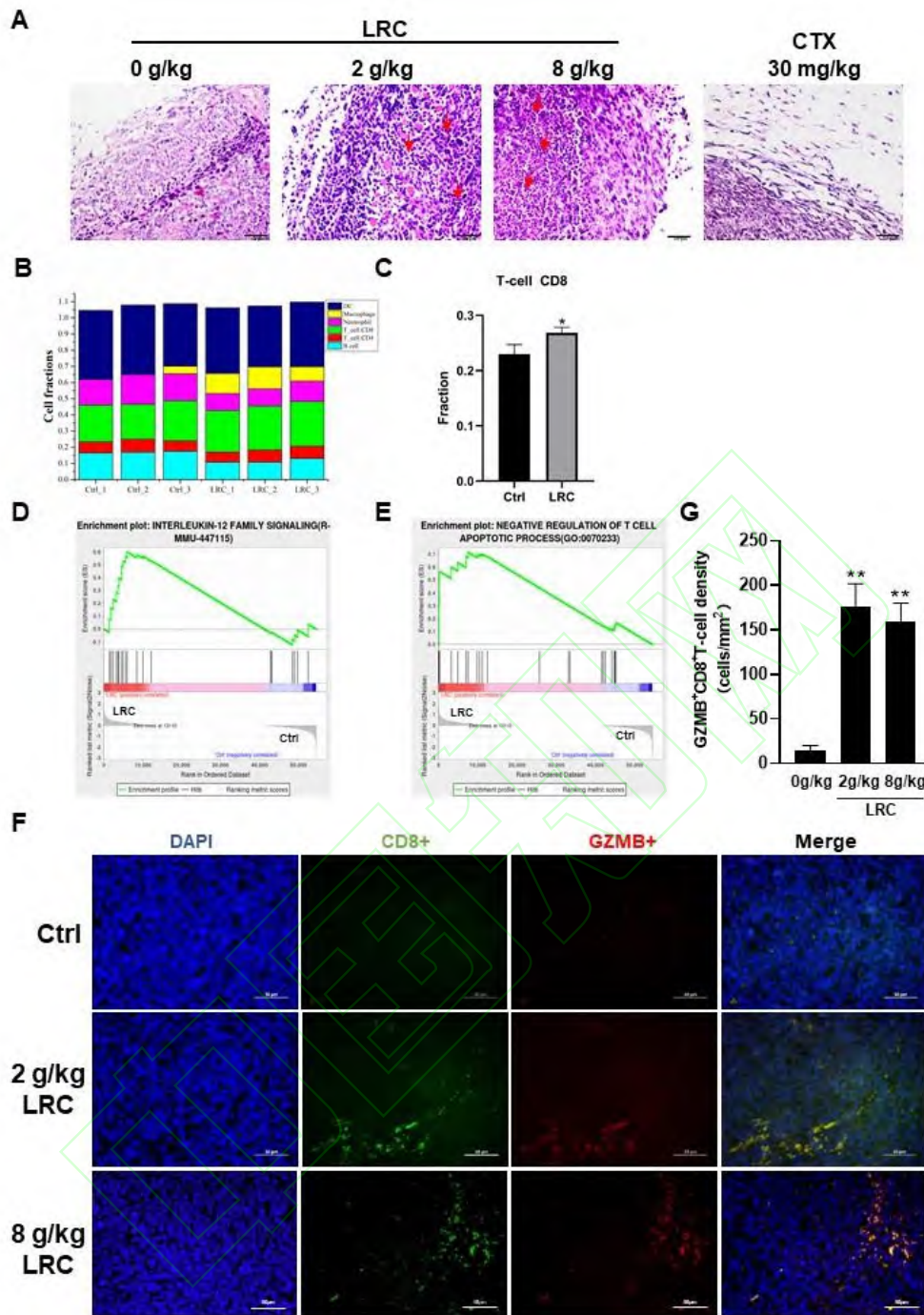


**Fig3.** LRC promotes CD8<sup>+</sup> T Cell infiltration and activity in tumors. (A) Pathological sections of LLC tumors stained with H&E showed that LRC promoted lymphocyte infiltration. The red arrows represent lymphocyte populations. (B, C) Tumor RNA sequencing and immune cell analysis using the TIMER database showed that LRC enhanced CD8<sup>+</sup> T cell infiltration. GSEA revealed that LRC promoted the IL-12 family signaling pathway (D) and negatively regulated the T lymphocytes apoptotic process (E) in tumors. (F) Immunofluorescence assay showed that LRC promoted the infiltration of CD8<sup>+</sup>GZMB<sup>+</sup> T lymphocytes in tumor tissue. (G) Bar graph showed the quantitative data of GZMB<sup>+</sup>CD8<sup>+</sup> T cells. These data were presented as the mean  $\pm$ SD, \*  $P < 0.05$ , \*\*  $P < 0.01$  vs. control group.

### 3.4. LRC affects the anti-tumor immune response through the PD-L1/PD-1 pathway

We then explored the mechanism of the effect of LRC on the anti-tumor immune response. Exploring the results of spleen GSEA, we found that the downstream pathways of PD-1, including RAS, MAPK, JAK-STAT, and PI3K-Akt signaling, were all up-regulated by the LRC treatment (Fig. 4A). On T lymphocytes membranes, PD-1 binds to its ligand PD-L1, leading to apoptosis [18], and the PD-L1/PD-1

pathway is associated with the infiltration of T cells into tumors [19]. Therefore, we hypothesized that the effects of LRC on anti-tumor immune response were mediated by the PD-L1/PD-1 pathway. We constructed a lung cancer cell line with stable PD-L1 overexpression (A549-PD-L1-OE, Fig. 4B), and co-cultured them with PBMCs in which T lymphocytes were activated *in vitro* with the CD3/CD28 antibody. PD-L1 overexpression significantly inhibited the killing effect of activated PBMCs on tumor cells, with the percentages of apoptotic A549-NC and A549-PD-L1-OE cells being 64% and 9%, respectively (Fig. 4C–D). We then found that 4 and 12  $\mu\text{g}/\text{mL}$  LRC reversed the effect of PD-L1 overexpression and improved the killing effect of activated PBMCs. As LRC had merely negligible impact on PBMC proliferation (Fig. 4E), these results reveal that the effect of LRC on anti-tumor immune response is mediated by the PD-L1/PD-1 pathway.

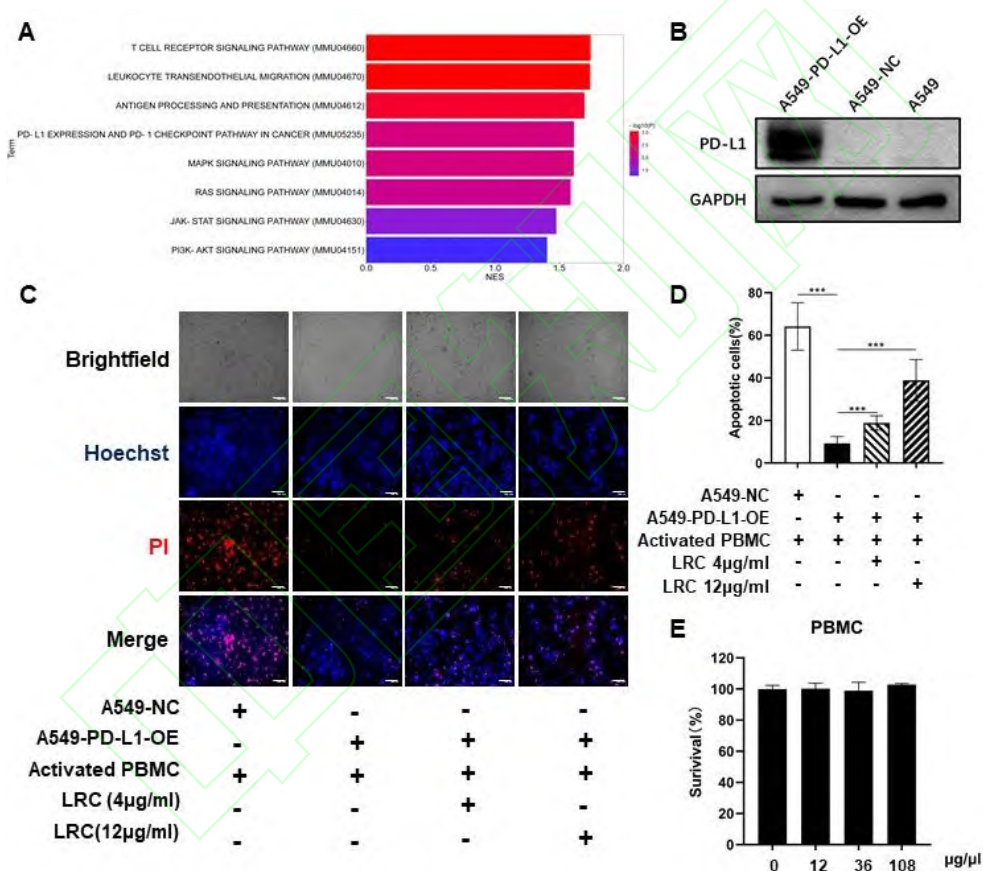


**Fig4.** LRC affects the anti-tumor immune response through the PD-L1/PD-1 pathway. (A) GSEA of spleen RNA sequencing data showed that LRC up-regulated PD-1 downstream signaling pathways. (B) Western blot showed that PD-L1 was over-expressed in the A549 cell line. A549-PD-L1-OE: A549 cells transfected with lentivirus carrying the PD-L1 gene. A549-NC: A549 cells transfected with empty lentivirus. (C) Effect of LRC on T cell tumor killing function. Representative images obtained by fluorescence microscopy. PBMCs activated by anti-CD3 and anti-CD8. (D) Statistical graph after image J recognition. The tumor cell apoptosis rate is the number of apoptotic tumor cells (Red fluorescence) divided by all the tumor cells in the field of vision (Blue fluorescence). (E) CCK8 showed that LRC had no effect on PBMC proliferation. These data were presented as the mean  $\pm$  SD, \*\*\* $P < 0.001$  vs. control group,  $n = 4$ .

### 3.5. LRC inhibited the PD-L1/PD-1 interaction by binding to PD-L1

The persistent expression of PD-L1 in A549-PD-L1-OE cells is exogenous, so the impact of LRC on the PD-L1/PD-1 pathway (Fig. 4C-D) at least partly depended on disrupting its function. Therefore, we assumed that LRC inhibited PD-L1/PD-1 binding. HTRF results confirmed that LRC blocked the interaction between PD-L1 and PD-1 with an  $\text{IC}_{50}$  of 519  $\mu\text{mol}/\text{L}$  (Fig. 5A). Next, we determined the  $K_D$  value of LRC and PD-L1

using BLI, and found a moderate affinity of 1.9  $\mu\text{mol/L}$  (Fig. 5B). These results indicate that LRC blocks the interaction between PD-L1 and PD-1 by binding to PD-L1. To confirm this finding, we established a cell model by stimulating Jurkat T with PHA, making them produce PD-1 (Fig. 5C); we then incubated the cells with the PD-L1 protein and, using flow cytometry, we found that PD-L1 enhanced the apoptosis of Jurkat T cells, while LRC effectively inhibited the PD-L1-mediated Jurkat T cell apoptosis induction (Fig. 5D). Employing western blot to detect Caspase 3, a crucial marker of apoptosis, also confirmed this finding (Fig. 5E). As PD-L1 binding to PD-1 leads to the phosphorylation of the cytoplasmic tail of PD-1 and the recruitment of p-SHP2, which dephosphorylates multiple downstream pathways and ultimately inhibits T cell activation [20,21], we then quantified p-SHP2 in Jurkat T cells after incubation with PD-L1. PD-L1 increased p-SHP2 levels, while LRC significantly reduced their PD-L1-induced increase (Fig. 5E). Considering that LRC had no inhibitory effect on the proliferation of Jurkat T cells (Fig. 5F), these results confirmed that LRC interacted with PD-L1, inhibiting PD-L1/PD-1 binding.

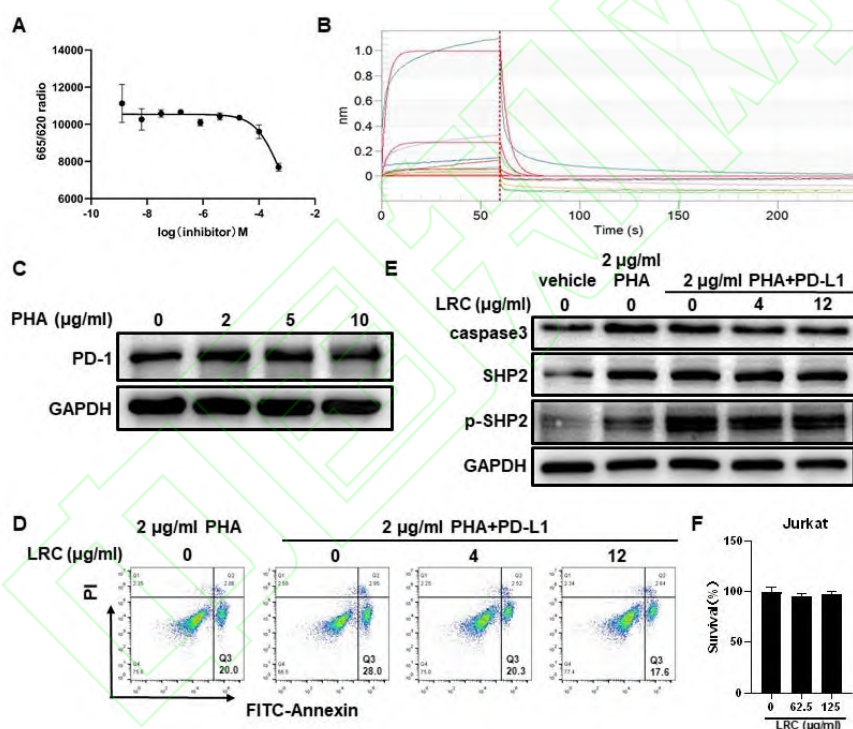


**Fig5.** LRC inhibited PD-1 and PD-L1 interaction by binding to PD-L1. (A) The HTRF assay showed that LRC inhibited PD-L1/PD-1 binding with an  $\text{IC}_{50}$  of 519  $\mu\text{mol/L}$ . (B) The binding dissociation curve determined by BLI analysis showed that LRC bound to PD-L1 with a  $K_D$  of 1.9  $\mu\text{mol/L}$ . (C) Western blot showed that PHA-stimulated PD-1 expression in Jurkat T cells at 2 and 5  $\mu\text{g/mL}$ . (D) Flow cytometry showed that LRC inhibited the PD-L1-induced apoptosis of Jurkat T cells. Jurkat T cells were stimulated with PHA to promote PD-1 expression and co-cultured with PD-L1 to induce apoptosis. (E) Western blot showed that LRC inhibited the up-regulation of caspase3, a crucial marker of apoptosis, and p-SHP2, a T cell suppressor activator and downstream protein of the PD-L1/PD-1 pathway, which were induced by PD-L1 in Jurkat T cells. (F) CCK8 showed that LRC had no significant impact on Jurkat T cells proliferation ( $n = 5$ ). These data were presented as the mean  $\pm$  SD.

#### 4. Discussion

Homologous medicine and food plants are especially popular in China due to their safety and health-promoting properties. LRC has documented hypolipidemic, hypotensive, hypoglycemic, and anti-osteoporotic effects [22], indicating its considerable healthcare value. LRC is routinely combined with

other herbs to form traditional Chinese medicine formulas used to treat various diseases. The formula composed of *Radix Glycyrrhizae*, *Cortex Mori*, and LRC is called Xie Bai San. It has been used to improve the clinical symptoms and quality of life of patients with advanced NSCLC, reduce adverse reactions, and prolong the survival of patients [14,23]. NSCLC development is highly dependent on the tumor immune microenvironment, and NSCLC cells interact with immune cells to promote immune escape [24]. The tumor immune escape mechanism is related to the induction of an immunosuppressive microenvironment and the inhibition of effector T cell function in the tumor microenvironment [25]. Removing the immunosuppressive microenvironment and/or restoring effector T cell function is of great significance for inhibiting tumor development. Although we documented the LRC-induced inhibition of the epithelial-mesenchymal transition [15], the effect and mechanism of LRC on tumor growth remain poorly understood.

In this study, we showed that LRC impeded tumor growth without hepatotoxicity and nephrotoxicity. LRC also displayed very low toxicity in other studies. Its reported median lethal dose by intraperitoneal injection is 12.8 g/kg in mice and 30 g/kg in dogs [26]. The maximum LRC dose used in mice was 20 g/kg, in an LPS-induced acute lung injury study [27]. We chose a dose of LRC based on our pre-experiments, which showed that 1 g/kg LRC had a slight anti-tumor effect on LLC-bearing mice. Consistent with our previous study, LRC does not inhibit the proliferation of NSCLC cells in humans and mice [15]. Given that the immunosuppressive microenvironment accelerates the growth of NSCLC, we hypothesized that LRC exerted its anti-tumor mechanism through immune regulation. We found that LRC increased the levels of the anti-tumor cytokines IFN- $\gamma$  and IL-2 in tumor-bearing mice serum, without affecting the number of CD8<sup>+</sup> and CD4<sup>+</sup> T lymphocytes in the spleen. There were some unexpected findings in the spleen GSEA. The activation of the TCR and Leukocyte transendothelial migration pathways were found to be highly associated with LRC treatment. This suggests that LRC activates anti-tumor immune responses and promotes T cell migration from the spleen to the tumor. In addition, we found that PD-1 downstream pathways, including RAS, MAPK, JAK-STAT, and PI3K-Akt signaling, were all up-regulated by LRC.

Based on these findings, we hypothesized that LRC plays an immunomodulatory role through the PD-L1/PD-1 pathway. PD-L1, an immune checkpoint with high expression in lung cancer, binds to PD-1 on the T lymphocytes membrane and recruits the cytoplasmic tyrosine phosphatase SHP-2 to the immunoreceptor tyrosine-based switch motif (ITSM), inhibiting T lymphocytes activity and IFN- $\gamma$  and IL-2 production [28]. The phosphorylation of SHP-2 contributes to the inhibitory signaling of the PD-L1/PD-1 pathway [29]. Traditionally, the prevailing belief was that PD-L1 primarily functioned within tumor tissues. However, emerging research has uncovered that tumor cells, particularly in NSCLC, can release PD-L1-rich exosomes [30]. These PD-L1-enriched exosomes possess the remarkable capacity to traverse the bloodstream and lymphatic system, thereby disseminating throughout the entire organism. As a result, they elicit a profound systemic immune suppression that significantly impacts crucial processes, such as lymph node drainage and spleen functionality [31]. PD-L1 antibody blockade or reduced PD-L1 expression can restore T lymphocyte proliferation and reduce the apoptosis by inhibiting this pathway [32]. We prepared an *in vitro*

co-culture cell model in which PD-L1 inhibited T cell killing activity. We found that LRC could restore the T cell killing activity that was inhibited by PD-L1. Then, the HTRF experiment uncovered that LRC blocked PD-L1/PD-1 binding and the BLI experiment proved that LRC bound to PD-L1. To confirm this, we co-incubated PHA-stimulated Jurkat T cells (thus expressing PD-1) and PD-L1 proteins, in the presence or absence of LRC. We assessed apoptosis using flow cytometry, and quantified Caspase 3 as a confirmatory marker and as an indicator of T cell apoptosis or exhaustion status [33,34]. LRC effectively reduced the PD-L1-induced apoptosis and pSHP2 up-regulation in Jurkat T cells. Besides, Jurkat T cells stimulated with a low dose of PHA produced more PD-1 than those treated with a high dose of PHA (Fig. 5C). These results may be due to the high apoptosis rate caused by high PHA doses. Collectively, these findings confirmed that LRC blocked the binding of PD-L1 and PD-1 by targeting PD-L1.

Some other plant extracts or natural products inhibit the PD-L1/PD-1 pathway. Notably, astragaloside [35,36], ginsenoside Rg3, cordycepin [37], and paeoniflorin [38], reduce the expression levels of PD-L1 or PD-1. Kim *et al.* found that *Geranii Herba* extract inhibited the PD-L1/PD-1 interaction with an  $IC_{50}$  of 87.93  $\mu\text{g}/\text{mL}$  (determined by competitive ELISA), and that the active ingredient kaempferol 7-O-rhamnoside bound to PD-L1 with a  $K_D$  value of 197  $\mu\text{mol}/\text{L}$  [39]. A *Salvia plebeia* extract also inhibited the PD-L1/PD-1 interaction, and the  $K_D$  value of the active ingredient cosmosiin with PD-L1 was 85  $\mu\text{mol}/\text{L}$  [40]. Next, a *Rhus Verniciflua Stokes* extract blocked the PD-L1/PD-1 interaction with an  $IC_{50}$  of 26.22  $\mu\text{g}/\text{mL}$ , and its compounds, eriodictyol, fisetin, quercetin, and liquiritigenin blocked the PD-1/PD-L1 interaction with  $IC_{50}$  values of 0.04, 0.04, 5.71, and 11.85  $\mu\text{mol}/\text{L}$ , respectively [41]. These reports indicate that the identification of PD-L1/PD-1 small molecule inhibitors from natural products is reliable and has therapeutic potential. In this study, we found that the  $K_D$  of LRC and PD-L1 binding was 1.9  $\mu\text{mol}/\text{L}$ , and LRC showed no obvious hepatorenal toxicity, indicating that it would be valuable to identify the compounds of LRC that inhibit PD-L1.

## 5. Conclusion

This study explored the anti-lung cancer effects of LRC and their mechanisms, and demonstrated that LRC bound to PD-L1 and blocked its interaction with PD-1, restoring the killing activity of T lymphocytes on tumor cells. These results provide an alternative strategy for the clinical treatment of lung adenocarcinoma, and may serve as a reference for further screening for natural small molecule inhibitors targeting PD-L1.

## Conflicts of interest

The authors have declared no conflict of interest.

## Acknowledgements

This study was supported by Natural Science Foundation of Guangdong Province, China (No.2022A1515011575), National Natural Science Foundation of China, China (No. 81873154) and President Foundation of Integrated Hospital of Traditional Chinese Medicine, Southern Medical University, China (No. 1202103010).

## References

- [1] K.C. Thandra, A. Barsouk, K. Saginala, et al., Epidemiology of lung cancer, *Wspolczesna Onkol.* 25 (2021) 45-52. <http://doi.org/10.5114/wo.2021.103829>.
- [2] S. Zhu, S. Zhao, Q. Zhang, et al., Complete disease remission in a tp53 and kras co-mutated brain oligometastatic lung cancer patient after immuno-chemotherapy and surgical resection: a case report, *Transl. Lung Cancer Res.* 10 (2021) 2298-2305. <http://doi.org/10.21037/tlcr-21-380>.
- [3] J.H. Kim, D.H. Kim, S. Jo, et al., Immunomodulatory functional foods and their molecular mechanisms, *Exp. Mol. Med.* 54 (2022) 1-11. <http://doi.org/10.1038/s12276-022-00724-0>.
- [4] K.V. Wissen, D. Blanchard, The use of vitamins and supplements for lung cancer prevention, *Am. J. Nurs.* 121 (2021) 21. <http://doi.org/10.1097/01.NAJ.0000737280.98335.3a>.
- [5] P. Krejbich, M. Birringer, The self-administered use of complementary and alternative medicine (cam) supplements and antioxidants in cancer therapy and the critical role of nrf-2-a systematic review, *Antioxidants* 11 (2022). <http://doi.org/10.3390/antiox11112149>.
- [6] J.Z. Chen, X. Lu, Y.Q. Hu, et al., Research progress on chemical constituents and pharmacological studies on root bark of *lycium barbarum*, *Zhongguo Zhong Yao Za Zhi* 46 (2021) 3066-3075. <http://doi.org/10.19540/j.cnki.cjmm.20210223.601>.
- [7] J.C. Jeong, S.J. Kim, Y.K. Kim, et al., Lycii cortex radice extract inhibits glioma tumor growth in vitro and in vivo through downregulation of the akt/erk pathway, *Oncol. Rep.* 27 (2012) 1467-1474. <http://doi.org/10.3892/or.2012.1637>.
- [8] X.H. Chen, L. Su, L.J. Jiang, et al., Identification of compounds in lycii cortex by uplc-ltq-orbitrap-ms, *Zhongguo Zhong Yao Za Zhi* 44 (2019) 4486-4494. <http://doi.org/10.19540/j.cnki.cjmm.20190506.202>.
- [9] X. Li, J. Lin, B. Chen, et al., Antioxidant and cytoprotective effects of kukoamines a and b: comparison and positional isomeric effect, *Molecules* 23 (2018). <http://doi.org/10.3390/molecules23040973>.
- [10] Q. Zhao, L. Li, Y. Zhu, et al., Kukoamine b ameliorate insulin resistance, oxidative stress, inflammation and other metabolic abnormalities in high-fat/high-fructose-fed rats, *Diabetes Metab. Syndr. Obes.* 13 (2020) 1843-1853. <http://doi.org/10.2147/DMSO.S247844>.
- [11] Q. Wang, H. Li, Z. Sun, et al., Kukoamine a inhibits human glioblastoma cell growth and migration through apoptosis induction and epithelial-mesenchymal transition attenuation, *Sci. Rep.* 6 (2016) 36543. <http://doi.org/10.1038/srep36543>.
- [12] M. Imran, G.T. Aslam, M. Atif, et al., Apigenin as an anticancer agent, *Phytother. Res.* 34 (2020) 1812-1828. <http://doi.org/10.1002/ptr.6647>.
- [13] J. Mottaghipisheh, H. Taghrir, D.A. Boveiri, et al., Linarin, a glycosylated flavonoid, with potential therapeutic attributes: a comprehensive review, *Pharmaceuticals* 14 (2021). <http://doi.org/10.3390/ph14111104>.
- [14] Z.H. Yang, Y.H. Qiu, C.M. Deng, Clinical observation on 32 cases of advanced non-small cell lung cancer treated with jiajian-xiebaisan combined with radiotherapy and chemotherapy, *J. Sichuan Tradit. Chin. Med.* 1 (2005) 36-37.
- [15] Z. Guo, H. Yin, T. Wu, et al., Study on the mechanism of cortex lycii on lung cancer based on network pharmacology combined with experimental validation, *J. Ethnopharmacol.* 293 (2022) 115280. <http://doi.org/10.1016/j.jep.2022.115280>.
- [16] A. Subramanian, P. Tamayo, V.K. Mootha, et al., Gene set enrichment analysis: a knowledge-based approach for interpreting genome-wide expression profiles, *Proc. Natl. Acad. Sci. U. S. A.* 102 (2005) 15545-15550. <http://doi.org/10.1073/pnas.0506580102>.
- [17] J.Q. Liu, C. Zhang, X. Zhang, et al., Intratumoral delivery of il-12 and il-27 mrna using lipid nanoparticles for cancer immunotherapy, *J. Control. Release* 345 (2022) 306-313. <http://doi.org/10.1016/j.jconrel.2022.03.021>.
- [18] H. Dong, S.E. Strome, D.R. Salomao, et al., Tumor-associated b7-h1 promotes t-cell apoptosis: a potential mechanism of immune evasion, *Nat. Med.* 8 (2002) 793-800. <http://doi.org/10.1038/nm730>.
- [19] H. Ahn, H.J. Lee, J.H. Lee, et al., Clinicopathological correlation of pd-11 and tet1 expression with tumor-infiltrating lymphocytes in non-small cell lung cancer, *Pathol. Res. Pract.* 11 (2020) 153188. <http://doi.org/10.1016/j.prp.2020.153188>.
- [20] M. Ramaswamy, T. Kim, D.C. Jones, et al., Immunomodulation of t- and nk-cell responses by a bispecific antibody targeting cd28 homolog and pd-11, *Cancer Immunol. Res.* 10 (2022) 200-214. <http://doi.org/10.1158/2326-6066.CIR-21-0218>.

- [21] Y. Song, M. Zhao, H. Zhang, et al., Double-edged roles of protein tyrosine phosphatase shp2 in cancer and its inhibitors in clinical trials, *Pharmacol. Ther.* 230 (2022) 107966. <http://doi.org/10.1016/j.pharmthera.2021.107966>.
- [22] E. Park, J. Kim, M.C. Kim, et al., Anti-osteoporotic effects of kukoamine b isolated from lycii radiceis cortex extract on osteoblast and osteoclast cells and ovariectomized osteoporosis model mice, *Int. J. Mol. Sci.* 20 (2019). <http://doi.org/10.3390/ijms20112784>.
- [23] W.H. Zhou, X. P. Huang, Y.F. Zhang, Effect of shenqi xiebai powder for survival quality and mentation of patients with advanced non-small-cell lung cancer, *Chin. Arch. Tradit. Chin. Med.* 32 (2014) 2507-2509. <http://doi.org/10.13193/j.issn.1673-7717.2014.10.063>.
- [24] A. Anichini, V.E. Perotti, F. Sgambelluri, et al., Immune escape mechanisms in non small cell lung cancer, *Cancers* 12 (2020). <http://doi.org/10.3390/cancers12123605>.
- [25] A. Thomas, G. Giaccone, Why has active immunotherapy not worked in lung cancer? *Ann. Oncol.* 26 (2015) 2213-2220. <http://doi.org/10.1093/annonc/mdv323>.
- [26] O. Potterat, Goji (*Lycium barbarum* and *L. Chinense*): phytochemistry, pharmacology and safety in the perspective of traditional uses and recent popularity, *Planta Med.* 76 (2010) 7-19. <http://doi.org/10.1055/s-0029-1186218>.
- [27] T.Z. Zhang, J.L. Zhang, B.B. Hao, *Lycium chinense* water extract attenuates acute lung injury induced by lipopolysaccharide in mice, *Chin. J. Exp. Tradit. Med.* 20 (2014) 147-150. <http://doi.org/10.13422/j.cnki.syfjx.2014220147>.
- [28] K. Sakuishi, L. Apetoh, J.M. Sullivan, et al., Targeting tim-3 and pd-1 pathways to reverse t cell exhaustion and restore anti-tumor immunity, *J. Exp. Med.* 207 (2010) 2187-2194. <http://doi.org/10.1084/jem.20100643>.
- [29] L. Ai, A. Xu, J. Xu, Roles of pd-1/pd-11 pathway: signaling, cancer, and beyond, *Adv. Exp. Med. Biol.* 1248 (2020) 33-59. [http://doi.org/10.1007/978-981-15-3266-5\\_3](http://doi.org/10.1007/978-981-15-3266-5_3).
- [30] D.H. Kim, H. Kim, Y.J. Choi, et al., Exosomal pd-11 promotes tumor growth through immune escape in non-small cell lung cancer, *Exp. Mol. Med.* 51 (2019) 1-13. <http://doi.org/10.1038/s12276-019-0295-2>.
- [31] M. Poggio, T. Hu, C.C. Pai, et al., Suppression of exosomal pd-11 induces systemic anti-tumor immunity and memory, *Cell* 177 (2019) 414-427. <http://doi.org/10.1016/j.cell.2019.02.016>.
- [32] Y. Wu, W. Chen, Z.P. Xu, et al., Pd-11 distribution and perspective for cancer immunotherapy-blockade, knockdown, or inhibition, *Front. Immunol.* 10 (2019) 2022. <http://doi.org/10.3389/fimmu.2019.02022>.
- [33] M.S. Guida, E.A. Abd, Y. Kafafy, et al., Thymoquinone rescues t lymphocytes from gamma irradiation-induced apoptosis and exhaustion by modulating pro-inflammatory cytokine levels and pd-1, bax, and bcl-2 signaling, *Cell Physiol Biochem.* 38 (2016) 786-800. <http://doi.org/10.1159/000443034>.
- [34] P.P. Liu, J.C. Zhu, G.X. Liu, et al., Salinomycin enhances the apoptosis of t-cell acute lymphoblastic leukemia cell line jurkat cells induced by vincristine, *Zhongguo Shi Yan XueYeXue Za Zhi* 23 (2015) 653-657. <http://doi.org/10.7534/j.issn.1009-2137.2015.03.010>.
- [35] X.L. Qu, Y. Zeng, L. Yao, Down-regulation of pd-1 and pd-11 expression by astragaloside iv inhibits invasion and migration of cervical cancer hela cells, *Immunol. J.* 34 (2018) 850-855. <http://doi.org/10.13431/j.cnki.immunol.j.20180131>.
- [36] S. Wang, J. Mou, L. Cui, et al., Astragaloside iv inhibits cell proliferation of colorectal cancer cell lines through down-regulation of b7-h3, *Biomed. Pharmacother.* 102 (2018) 1037-1044. <http://doi.org/10.1016/j.biopha.2018.03.127>.
- [37] Q. An, L.W. He, H.Y. Wu, Mechanism of cordycepin promotes tumor immunity by regulating PD-1 receptor of CD4+T lymphocytes, *J. Nanjing Univ. Tradit. Chin. Med.* 34 (2018) 495-498. <http://doi.org/10.14148/j.issn.1672-0482.2018.0495>.
- [38] N.Y. Wan, C.H. Jiang, M. Gao, Paeoniflorin inhibits programmed cell death-1- ligand 1 expression in hepg2 cells by regulating jak/stat3 signal pathway, *J. China Pharm. Univ.* 50 (2019) 213-221. <http://doi.org/10.11665/j.issn.1000-5048.20190213>.
- [39] J.H. Kim, Y.S. Kim, J.G. Choi, et al., Kaempferol and its glycoside, kaempferol 7-o-rhamnoside, inhibit pd-1/pd-11 interaction in vitro, *Int. J. Mol. Sci.* 21 (2020). <http://doi.org/10.3390/ijms21093239>.
- [40] J.G. Choi, Y.S. Kim, J.H. Kim, et al., Anticancer effect of salvia plebeia and its active compound by improving t-cell activity via blockade of pd-1/pd-11 interaction in humanized pd-1 mouse model, *Front. Immunol.* 11 (2020) 598556. <http://doi.org/10.3389/fimmu.2020.598556>.

- [41] W. Li, T.I. Kim, J.H. Kim, et al., Immune checkpoint pd-1/pd-11 ctla-4/cd80 are blocked by rhus verniciflua stokes and its active compounds, *Molecules* 24 (2019). <http://doi.org/10.3390/molecules24224062>.

